International Journal of Pharmaceutics 458 (2013) 48–56

Contents lists available at ScienceDirect

International Journal of Pharmaceutics

journal homepage: www.elsevier.com/locate/ijpharm

Pharmaceutical Nanotechnology

Targeted gene delivery to glioblastoma using a C-end rule RGERPPR peptide-functionalised polyethylenimine complex

Jing Wang[a], Yang Lei[a], Cao Xie[a], Weiyue Lu[a], Zhiqiang Yan[b], Jie Gao[a], Zuoxu Xie[a], Xiaoyu Zhang[a], Min Liu[a,*]

[a] Key Laboratory of Smart Drug Delivery (Fudan University), Ministry of Education, Department of Pharmaceutics, School of Pharmacy, Fudan University, 826 Zhangheng Road, Shanghai 201203, PR China
[b] National Engineering Research Center for Nanotechnology, Shanghai 200241, PR China

ARTICLE INFO

Article history:
Received 1 August 2013
Accepted 3 October 2013
Available online 19 October 2013

Keywords:
Glioma targeting
C-end rule peptide
Neuropilin-1
Gene delivery
Polyethylenimine

ABSTRACT

Safe and efficient systems capable of specifically targeting brain tumour cells represent a promising approach for the treatment glioblastoma multiforme. Neuropilin-1 (NRP-1) is over-expressed in U87 glioma cells. In the current study, the tumour specific peptide RGERPPR, which binds specifically to NRP-1, was used as a targeting ligand in a gene delivery strategy for glioblastoma. The RGERPPR peptide was coupled to branched polyethylenimine (PEI, 25 kDa) using heterobifunctional Mal–PEG–NHS, resulting in a novel gene delivery polymer. Polymer/plasmid DNA (pDNA) complexes were formed and their sizes and zeta potentials were measured. Compared with the unmodified mPEG–PEI/pDNA complexes, the RGERPPR–PEG–PEI/pDNA complex led to a significant enhancement in intracellular gene uptake and tumour spheroid penetration. Furthermore, the RGERPPR–PEG–PEI/pDNA complex facilitated enhanced transfection efficiency levels, as well as a reduction in cytotoxicity when tested in U87 glioma cells in vitro. Most significantly of all, when complexes formed with pDsRED-N1 were injected into the tail vein of intracranial U87 tumour-bearing nude mice, the RGERPPR–PEG–PEI complexes led to improved levels of red fluorescence protein expression in the brain tissue. Taken together, the results show that RGERPPR–PEG–PEI could be used as a safe and efficient gene delivery vehicle with potential applications in glioblastoma gene delivery.

1. Introduction

Glioblastoma multiforme (GBM) is the most common and aggressive malignant brain tumour, and accounts for approximately 40% of all brain tumour cases (Lopes, 2003; Meyer, 2008). GBM has been shown to be highly proliferative, infiltrative and invasive (Gladson et al., 2010), and these properties of the disease make it difficult for treatment strategies involving clinical surgery, chemotherapy or radiotherapy to be used effectively to provide significant improvements in survival. The use of gene therapy for the treatment of brain tumours has therefore become the subject of considerable interest from research working in this particular area of cancer (Zhan et al., 2012; Bai et al., 2013; Murphy and Rabkin, 2013). Several factors are known to make the treatment of brain tumours particularly challenging, including the blood–brain barrier (BBB), and the lesser known blood–tumour barrier (BTB), which can both limit or even prevent the accumulation and uptake of drugs in the areas that they are needed for the treatment of brain tumours (Groothuis, 2000; Pardridge, 2002). Brain tumour cell-specific targeting systems represent a promising strategy to address the issues imposed by the BTB. Researchers have reported a variety of different targeting ligands, including the GMT8 aptamer (Gao et al., 2012a,b), AS1411 aptamer (Gao et al., 2012a,b), cyclic RGD (Merkel et al., 2009; Mickler et al., 2011), MT1-AF7p peptide (Gu et al., 2013), and F3 peptide (Hu et al., 2013), which can bind specifically and efficiently to brain tumour cells to establish the brain glioma delivery systems.

Neuropilin-1 (NRP-1) is a type I transmembrane glycoprotein and a coreceptor for class semaphorin-3A (He and TessierLavigne, 1997; Kolodkin et al., 1997; Takahashi et al., 1999) and vascular endothelial growth factor (Soker et al., 1998; Oh et al., 2002; Soker et al., 2002), and mediates a variety of critical functions during angiogenesis, the regulation of vascular permeability, and the development of the nervous system. NRP-1 has been reported to be over-expressed in several tumour cells, including glioblastoma cells (Osada et al., 2004; Nasarre et al., 2010; Li et al., 2011), and therefore represents an attractive candidate to be used for the development of a delivery system for the treatment of GBM. Peptides containing the C-terminal motif R/KXXR/K (R, arginine; K, lysine; X, any amino acid), which are otherwise known as C-end rule

* Corresponding author. Tel.: +86 21 51980092; fax: +86 21 51980090.
E-mail addresses: liumin@shmu.edu.cn, liumin1996@gmail.com (M. Liu).

0378-5173/$ – see front matter © 2013 Elsevier B.V. All rights reserved.
http://dx.doi.org/10.1016/j.ijpharm.2013.10.017

(CendR) peptides, were discovered using phage-displayed libraries, and show a high level of binding affinity to the NRP-1 receptor. Importantly, CendR peptides can also induce extravasation and tissue penetration, and this can help to overcome high levels of interstitial pressure in tumours (Teesalu et al., 2009). Researchers have designed the novel tumour-penetrating peptides iRGD and tLyP-1 using a conventional αv integrin-binding RGD peptide and a p32-binding LyP-1 peptide, respectively, as well as a CendR peptide that had been proteolytically cleaved. The iRGD and tLyP-1 peptides have both been reported to exhibit tumour-homing and tissue-penetrating properties, as well as being able to efficiently deliver drugs and nanoparticles into the tumour parenchyma (Sugahara et al., 2009; Roth et al., 2012). It has also been reported that the co-administration of iRGD or tLyP-1 enhanced the treatment efficiency of cancer drugs and particles (Sugahara et al., 2010; Hu et al., 2013). There have been no reports, however, concerning the use of CendR peptides in gene delivery to improve the transfection efficiency of different vectors. Furthermore, there have not been any reports concerning the use of CendR peptides for the treatment of GBM. Herein, we report the use of the CendR peptide RGERPPR as a tumour homing and penetrating peptide to mediate site-specific accumulation and enhance transfection efficiency in the gene therapy of GBM.

The availability of a safe and efficient delivery vehicle is an important requirement for gene therapy. Polyethylenimine (PEI) is considered to be one of the most successful and efficient non-viral vectors, and also has a high gene transfection efficiency. PEI has a high cationic charge that facilitates the efficient condensation of DNA. Furthermore, PEI can trigger the endosomal release of the complexes into the cytoplasm via the 'proton sponge' effect (Boussif et al., 1995; Godbey et al., 1999). Unfortunately, however, PEI still suffers from inherent toxicity because of its high positive charge and non-selective delivery, and these factors have ultimately limited its application in vivo. It has been reported that the attachment of polyethylene glycol (PEG) could reduce the toxicity of PEI, as well reducing its plasma protein binding, improving its biocompatibility, and prolonging its circulation in the blood (Ogris et al., 1999; Nguyen et al., 2000; Kleemann et al., 2005).

In the current work, we have synthesised an RGERPPR modified PEG–PEI glioblastoma-targeted gene delivery system, and the formation of the resulting polymer was confirmed by ^{1}H NMR analysis. Following the formation of the polymer/pDNA complexes, dynamic light scattering was used to evaluate their size and zeta potential properties. The U87 glioma cell uptake, tumour spheroid penetration, in vitro cytotoxicity and transfection efficiency properties of the complexes were also evaluated. An intracranial U87 tumour-bearing nude mice model was established and used in conjunction with a red fluorescence protein assay to confirm the targeting efficacy of the RGERPPR–PEG–PEI gene delivery system in vivo.

2. Materials and methods

2.1. Materials

High molecular weight PEI (branched, M_W: 25,000) was purchased from Sigma–Aldrich (Munich, Germany). CH_3O–PEG–Mal (mPEG–Mal, M_W: 2000) and Mal–PEG–NHS (M_W: 2000) were obtained from Jenkem Technology (Beijing, China). RGERPPR were purchased from ChinaPeptides Co. Ltd. (Shanghai, China). Tissue-tek optimal cutting temperature (OCT) embedding medium was supplied by Sakura Finetek (Torrance, CA, USA). A luciferase assay kit was purchased from Promega (Beijing, China). A BCA (bicinchoninic acid) protein assay kit was from Beyotime (Shanghai, China). TOTO®-3 dye was purchased from Life Technologies (Shanghai, China). The plasmid DNA encoding EGFP (pEGFP-N2) and RFP (pDsRED-N1) were purchased from Genechem Co. (Shanghai, China) and the $pGL_{4.2}$ luciferase reporter gene plasmid were purchased from Promega. All of the plasmid DNAs used in the current study was used following their purification with a QIAGEN Plasmid Mega Kit (Qiagen GmbH, Hilden, Germany). Phosphate-buffered saline (PBS), Dulbecco's modified Eagle's medium (DMEM), foetal bovine serum (FBS), trypsin–EDTA (0.25%), penicillin–streptomycin and agarose were purchased from Gibco (Invitrogen, USA). The U87 glioma cells were obtained from the Shanghai Institute of Cell Biology, and cultured in DMEM containing 10% FBS, 100 U/mL penicillin and 100 mg/mL streptomycin under a humidified atmosphere of 5% CO_2/air at 37 °C.

2.2. Synthesis of methoxy poly(ethylene glycol)–polyethylenimine (mPEG–PEI)

A solution of mPEG–Mal (10 μmol) in dimethyl sulfoxide (DMSO; 100 μL) was added to a solution of PEI (2 μmol) in PBS (2 mL, 0.2 M, pH 7.4), and the resulting mixture was stirred overnight at ambient temperature. The mixture was then added to an Amicon Ultra filter tube (MWCO: 10,000 Millipore) and washed five times with distilled water (dH_2O). The mPEG–PEI product was then lyophilised for further use.

2.3. Synthesis of RGERPPR–polyethylenimine–poly(ethylene glycol) (RGERPPR–PEG–PEI)

The amino group of RGERPPR was initially coupled to the NHS group of Mal–PEG–NHS to give RGERPPR–PEG–Mal, which was then conjugated with PEI using the maleimide-amino reaction to obtain the final conjugate.

The RGERPPR peptide was synthesised using solid phase peptide synthesis and purified by HPLC. A solution of triethylamine (3 μL, TEA) in dimethyl formamide (300 μL, DMF) was added to a solution of Mal–PEG–NHS (10 μmol) and RGERPPR (13 μmol) in DMF (1 mL) in a drop-wise manner, and the resulting mixture was stirred at ambient temperature for 1 h to give the desired product, which was purified using an ÄKTA explorer 100 system (GE, Fairfield, CT, USA) on a SephadexG-15 column (GE). The RGERPPR–PEG–Mal product was subsequently obtained through lyophilisation.

The RGERPPR–PEG–PEI was synthesised as follows. A 5-fold molar excess of RGERPPR–PEG–Mal was added to a solution of PEI (1.2 μmol) in PBS (1.5 mL, 0.2 M, pH 7.4), and the resulting mixture was stirred overnight before being purified by dialysis against dH_2O in an Amicon Ultra filter tube five times. The resulting product was then collected and lyophilised.

2.4. Polymer characterisation

The mPEG–PEI and RGERPPR–PEG–PEI polymers synthesised in the current study were characterised by ^{1}H NMR analysis using D_2O as the solvent on a 500 MHz NMR spectrometer (Varian, Palo Alto, CA, USA).

2.5. Polymer/pDNA complex preparation

The polymer/pDNA complexes were formed via the drop-wise addition of equal volumes of varying concentrations of the polymer solution to a pDNA solution (80 μg/mL) dissolved in PBS (pH 7.4). The concentrations of the polymer solutions were dependent on the *N*/*P* ratios (i.e., the polymer amine to DNA phosphate ratios). The resulting complexes were immediately vortexed for 30 s before being incubated at 37 °C for 30 min.

2.6. Size and zeta potential measurements

The sizes and zeta potentials of the polymer/$pGL_{4.2}$ complexes with different *N*/*P* ratios were monitored using dynamic light scattering (Zetasizer Nano ZS, Malvern Instruments, Worcestershire, UK). Three measurements were performed on each sample, and the results are presented as the mean value ± SD.

2.7. Cytotoxicity assay

U87 glioma cells were seeded in 96-well plates at a density of 5, 000 cells/well in 200 μL of DMEM containing 10% FBS, and incubated overnight. Twenty microliters of freshly prepared PEI/$pGL_{4.2}$, mPEG–PEI/$pGL_{4.2}$ and RGERPPR–PEG–PEI/$pGL_{4.2}$ complexes with different *N*/*P* ratios were then added to each well (0.8 μg $pGL_{4.2}$/well). After 12 h of incubation, the medium was exchanged with fresh DMEM, and the cells were incubated for 48 h. Twenty microliters of an MTT solution (5 mg/mL) was then added to each well, and the resulting mixtures were incubated for 4 h. The medium was then removed, and 150 μL of DMSO was added to dissolve the formazan crystals. After 15 min of incubation with DMSO, measurements were performed at a wavelength of 490 nm using a microplate reader (PowerWave XS, Bio-TEK, Winooski, VT, USA). The resulting data are expressed as the mean values ± SD of three measurements.

2.8. Cellular uptake

The plasmid DNA ($pGL_{4.2}$) was labelled with TOTO®-3 dye as described in a protocol provided by the manufacturer (Life Technologies, Shanghai, China). Briefly, 1 μL of the TOTO®-3 stock solution was diluted in 9 μL of dH_2O, and 125 μL (50 μg) of pDNA was added to the resulting dye solution. The mixture was then vortexed for 2 min before being incubated in the absence of light for 8 min. PBS (490 μL) was then added to a final concentration of 50 μg of pDNA in 625 μL of PBS.

U87 glioma cells were seeded in 48-well plates (20,000 cells/well) in 0.5 mL of DMEM with 10% FBS and incubated overnight. Freshly prepared RGERPPR–PEG–PEI/$pGL_{4.2}$ and mPEG–PEI/$pGL_{4.2}$ complexes with an *N*/*P* ratio of 12 were added into the 48-well plate with 2 μg of TOTO®-3 labelled pDNA per well, and the resulting mixtures were incubated with FBS for 4 h. The U87 glioma cells were then washed twice with PBS before being fixed with 4% formaldehyde for 15 min, and then stained with DAPI solution for 10 min. The fluorescence images were acquired and photographed using a fluorescence microscope.

2.9. Tumour spheroid penetration

The plasmid DNA ($pGL_{4.2}$) was labelled with TOTO®-3 dye, as described above. For further evaluation of the tumour-penetrating ability of the RGERPPR–PEG–PEI/$pGL_{4.2}$ complex, U87 cells were seeded in 48-well plates (2000 cells/400 μL per well) precoated with 150 μL of 2% low-melting-temperature agarose to prepare the three-dimensional tumour spheroids. Seven days later, 50 μL (containing 2 μg) of freshly prepared RGERPPR–PEG–PEI/$pGL_{4.2}$ and mPEG–PEI/$pGL_{4.2}$ complexes with an *N*/*P* ratio of 12 were incubated with the tumour spheroids for 12 h. The spheroids were then rinsed with ice-cold PBS before being fixed with 4% paraformaldehyde for 0.5 h and observed with a laser scanning confocal microscope (SP5, Leica, Germany).

2.10. In vitro transfection efficiency

2.10.1. Enhanced green fluorescence protein assay

U87 glioma cells were seeded in 48-well plates (20,000 cells/well) in 0.5 mL of DMEM containing 10% FBS 24 h prior to the experiment. The medium was then replaced with fresh DMEM (containing 10% FBS), and 50 μL of the polymer/pEGFP-N2 complexes (containing 2 μg pEGFP-N2, with an *N*/*P* of 12) were added to each well. Following a 12 h period of incubated at 37 °C, the medium was changed and the cells were incubated for a further 48 h. The fluorescence images were then visualised with a fluorescence microscope (Leica, DMI4000B, Wetzlar, Germany) and quantified by Flow Cytometry on a FACS CantoTM Π (BD Biosciences, San Jose, CA, USA).

2.10.2. Luciferase assay

Freshly prepared polymer/$pGL_{4.2}$ complexes with a variety of different *N*/*P* ratios were added to the U87 glioma cells according to the procedure described above and the resulting gene expression levels were quantified using a luciferase assay. Following the incubation, the luciferase activity was measured using a luciferase assay kit, and the relative light units (RLUs) were evaluated using an ultra-weak luminescence analyser (Chuanghe, Beijing, China). The amount of protein was measured with a BCA Protein Assay Kit. Three measurements were performed on each sample and data were expressed in RLU/mg protein (±SD).

2.11. Animal model establishment

Male BALB/c nude mice of 4–6 weeks of age were obtained from Shanghai SLAC Laboratory Animal Co. Ltd. (Shanghai, China) and kept under SPF conditions. All of the animal experiments conducted in the current study were evaluated and approved by the Ethics Committee of Fudan University. Nude mice (4–6 weeks of age) were used to establish the intracranial glioblastoma model. Briefly, 5 μL of U87 glioma cells in PBS (containing 600,000 cells) were implanted into the right striatum (1.8 mm lateral, 0.6 mm anterior to the bregma and 3.0 mm in depth) of nude mice using a stereotactic fixation device with a mouse adaptor. For confirmation of the establishment of the animal model, the brains were hydrated in 20% and 30% sucrose solutions until subsidence after they had been fixed in 4% paraformaldehyde for 1 day. The frozen brains prepared in OCT embedding medium at −80 °C were cut into 20 μm thick slices with a cryotome Cryostat (Leica, CM 1900, Wetzlar, Germany) and stained with haematoxylin–eosin for 10 min at ambient temperature. The sections were then measured using the fluorescence microscope after being washed twice with PBS.

2.12. In vivo transfection efficiency

The polymer/pDsRED-N1 complexes with an *N*/*P* ratio of 12 were prepared to evaluate the gene expression in the brains of intracranial U87 glioblastoma-bearing nude mice. The randomly assigned mice were anaesthetised and sequentially injected with 40 μg of pDsRED-N1 in 200 μL of PBS via the tail vein ($n = 3$). This process was repeated 3 times at 13, 15, and 17 days after the implantation. On the second day after the last administration, the mice were anaesthetised with 10% chloral hydrate, exsanguinated with a saline solution and fixed with 4% paraformaldehyde. Their brains were then excised and the amount of red fluorescence protein was measured using a Kodak FX Pro fluorescent imaging system (Rochester, NY, USA).

3. Results

3.1. Synthesis and characterisation of mPEG–PEI and RGERPPR–PEG–PEI

The RGERPPR–PEG–PEI was constructed using a two-step synthesis based on a heterobifunctional PEG linker (Mal–PEG–NHS), as shown in Scheme 1. The results of the ^{1}H-NMR spectra (Fig. 1)

Table 1
Molecular compositions of mPEG–PEI and RGERPPR–PEG–PEI.

Polymer	SD[a] of PEG		M_w (kDa)	
	Theoretical	Calculated	Theoretical	Calculated
mPEG–PEI	5.0	4.3	35.0	33.6
RGERPPR–PEG–PEI	5.0	4.4	38.8	37.1

[a] SD, substituted degree.

were as follows: 2.5–3.2 ppm (m, $-CH_2CH_2NH-$) for PEI, 3.6–3.9 (m, $-OCH_2CH_2$) for PEG and 3.95 (d, 2H, CH) and 4.15 (s, H, CH) for RGERPPR. The peaks at 3.95 and 4.15 ppm were present in the NMR spectrum of RGERPPR–PEG–PEI, suggesting that the targeted polymer had been synthesised successfully. Based on the ratios of the integrals for the characteristic peaks of the PEI and PEG backbones, we were able to calculate the degrees of substitution and molecular weights of mPEG–PEI and RGERPPR–PEG–PEI (Table 1).

3.2. Sizes and zeta potentials of the polymer/pDNA complexes

The sizes and zeta potentials of the polymer/$pGL_{4.2}$ complexes are shown in Table 2. In almost all of the complexes, the sizes decreased and the zeta potentials increased as the *N*/*P* ratios increased because of the stronger condensation ability of PEI (Lungwitz et al., 2005; Neu et al., 2005). All of the polymers had positive zeta potentials over the *N*/*P* ratios tested, with PEI exhibiting the highest surface charges. In contrast, the hydrophilic spacer PEG reduced the positive charges of the mPEG–PEI/$pGL_{4.2}$ and RGERPPR–PEG–PEI/$pGL_{4.2}$ complexes. Interestingly, when the *N*/*P* ratios were greater than 4, the particle sizes of the PEI/$pGL_{4.2}$ complexes (25 kDa) were in the range of 300–900 nm, whereas the sizes of the complexes formed from the PEGylated PEI had been reduced significantly (<265 nm). These observations could be explained by the small particles aggregating into large particles in the high ionic strength media. The PEGylation could reduce the surface charge of the PEI and lead to a reduction in the level of aggregation (Neu et al., 2007; Luo et al., 2010). The modification of the targeting peptide RGERPPR led to only minor changes in the zeta potential and size properties.

Table 2
Sizes and zeta potentials of the polymer/pGL4.2 complexes with different *N*/*P* ratios.

Sample	*N*/*P*	Size (nm)	Zeta potential (mV)
PEI	4	1496.3 ± 88.0	26.43 ± 0.62
	8	905.6 ± 119.3	35.47 ± 0.50
	12	527.2 ± 48.1	40.87 ± 0.57
	16	304.4 ± 24.9	43.73 ± 0.41
mPEG–PEI	4	1910.7 ± 47.3	4.23 ± 0.56
	8	260.0 ± 2.3	7.42 ± 0.23
	12	214.8 ± 0.3	10.43 ± 0.12
	16	207.9 ± 0.2	11.40 ± 0.08
RGERPPR–PEG–PEI	4	1755.7 ± 79.7	3.96 ± 0.38
	8	219.4 ± 2.8	4.40 ± 0.47
	12	179.4 ± 0.1	5.84 ± 0.49
	16	163.2 ± 0.3	8.09 ± 0.01

Data points represent the mean ± SD ($n = 3$).

3.3. Cytotoxicity assay

Cytotoxicity is an important factor for consideration when selecting polymeric gene vectors. An in vitro MTT assay was conducted to evaluate the cytotoxicities of the complexes in U87 glioma cells (Fig. 2). When the *N*/*P* ratio was greater than eight, the PEI/$pGL_{4.2}$ complexes exhibited an increased cytotoxicity. These results were attributed to the highly positive charges of the PEI/$pGL_{4.2}$ complexes. In contrast, the mPEG–PEI/$pGL_{4.2}$ and

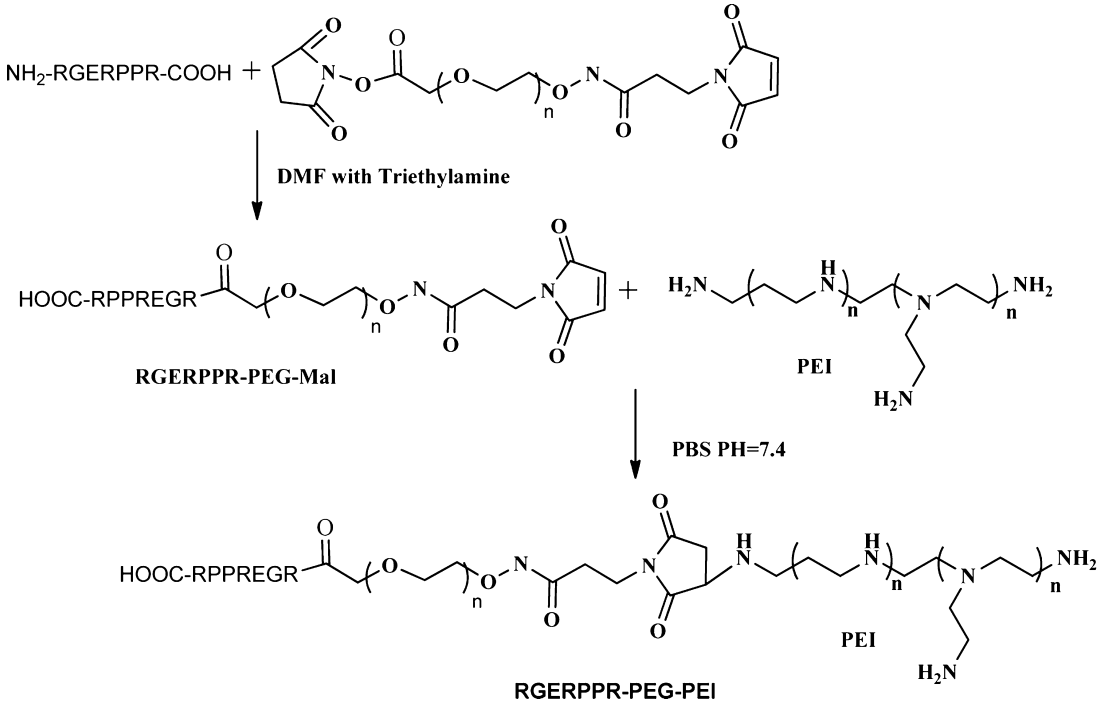

Scheme 1. Synthesis of RGERPPR–PEG–PEI.

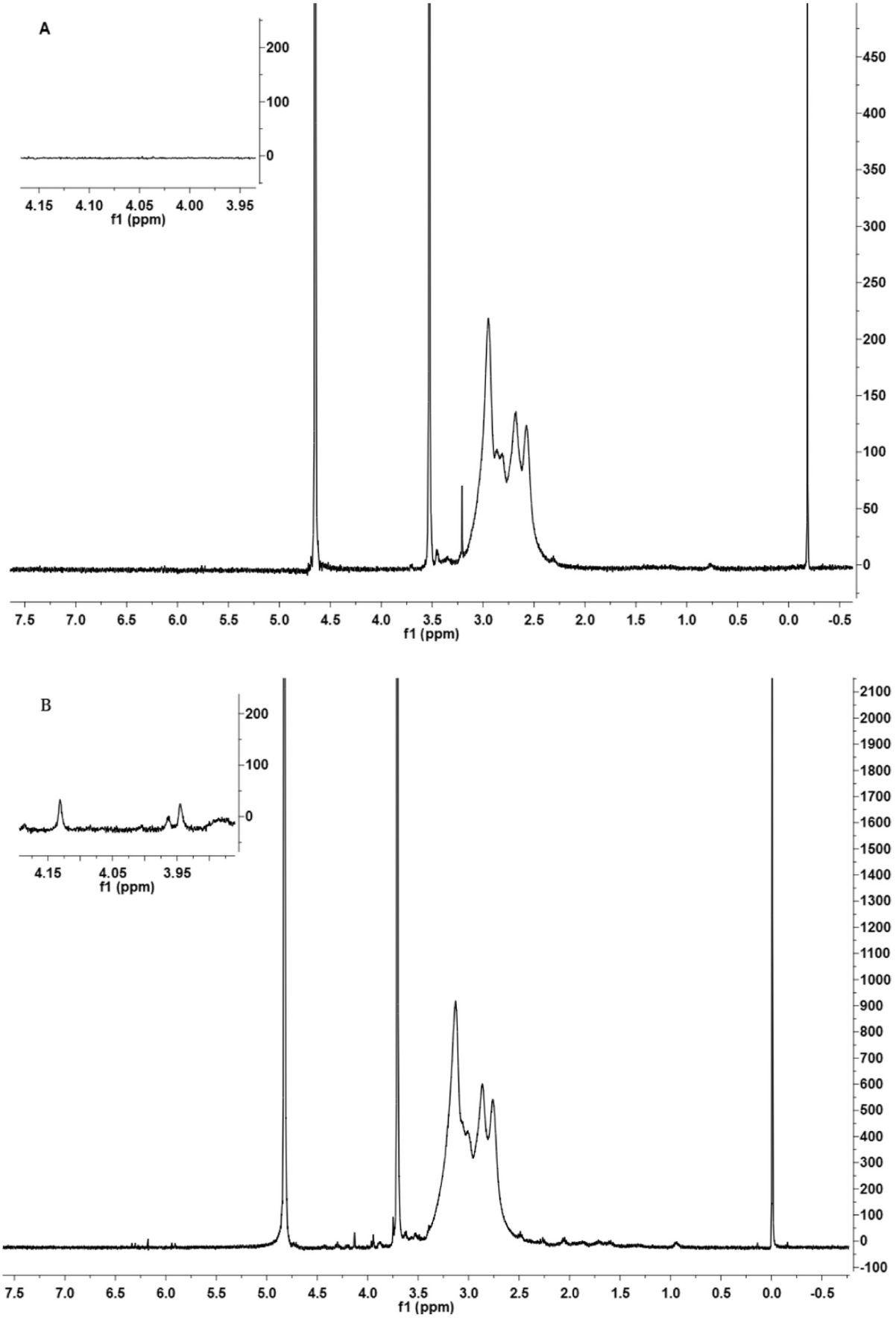

Fig. 1. ^{1}H-NMR spectra of (A) mPEG–PEI and (B) RGERPPR–PEG–PEI in D_2O.

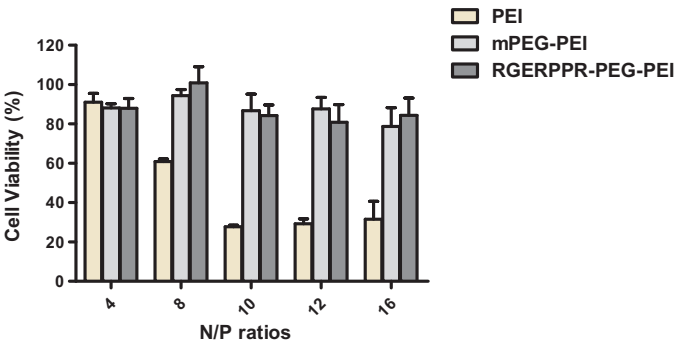

Fig. 2. Cell viabilities of mPEG–PEI/pEGFP-N2 and RGERPPR–PEG–PEI/pEGFP-N2 in comparison with PEI/pEGFP-N2 in U87 glioma cells.

RGERPPR–PEG–PEI/pGL$_{4.2}$ complexes showed the lowest cytotoxicities and the highest cell viabilities (greater than 80%) of the *N*/*P* ratios tested in the current study. On the basis of these results, an *N*/*P* ratio of 8 was selected for the PEI, whereas an *N*/*P* ratio of 12 was selected for the PEGylated PEI.

3.4. Cellular uptake

The cellular uptake of the TOTO®-3-labelled pDNA complexed with mPEG–PEI and RGERPPR–PEG–PEI by the U87 glioma cells was evaluated by fluorescence microscopy (Fig. 3). At an *N*/*P* ratio of 12 and an incubation time of 4 h, the TOTO®-3-labelled DNA from both groups was distributed in the cytoplasm or the nuclei. Compared with mPEG–PEI/pGL$_{4.2}$, the red fluorescence intensity of the RGERPPR–PEG–PEI/pGL$_{4.2}$ was much higher and therefore indicated a more efficient level of internalisation by the U87 glioma cells. These results indicated that the RGERPPR peptide performed an active targeting role in the uptake of the RGERPPR–PEG–PEI/pGL$_{4.2}$ complex by the U87 cells in vitro.

3.5. Tumour spheroid penetration

The tumour spheroids were used to imitate the in vivo status of solid tumours and evaluate the penetrating ability of the RGERPPR–PEG–PEI/pGL$_{4.2}$ complex by confocal microscopy. As shown in Fig. 4, the penetration of the RGERPPR–PEG–PEI/pGL$_{4.2}$ complex was much deeper and its distribution and fluorescence intensity properties were much higher than those of PEG–PEI/pGL$_{4.2}$ in the U87 tumour spheroids. These results indicated that the RGERPPR peptide could be used to effectively increase the tumour penetration efficacy which could play an important role in improving gene delivery.

3.6. In vitro transfection efficiency

The in vitro transfection efficiencies of the different polymers towards the U87 glioma cells were evaluated using the pEGFP-N2 and pGL$_{4.2}$ reporter gene systems. PEI (25 kDa) was used as control with the optimal *N*/*P* ratio of 8.

An enhanced green fluorescent protein expression assay was initially performed with fluorescence microscopy. As shown in Fig. 5A and B, the mPEG–PEI/pEGFP-N2 and RGERPPR–PEG–PEI/pEGFP-N2 complexes were both capable of transferring in U87 glioma cells. Importantly, following the attachment of the RGERPPR peptide, the EGFP expression was enhanced from 12.9% to 19.6%, as determined by flow cytometry (Fig. 5C). A luciferase assay was conducted to quantify the transfection efficiency of RGERPPR–PEG–PEI. Fig. 6 clearly shows that at an *N*/*P* ratio of 12, the RGERPPR–PEG–PEI/pGL$_{4.2}$ complex exhibited a 1.9-fold increase in luciferase expression relative to mPEG–PEI/pGL$_{4.2}$ ($P < 0.05$), and even had a comparable effect to that of PEI (*N*/*P* = 8).

3.7. Animal model establishment and in vivo transfection efficiency

In the images of the frozen brain sections of an intracranial U87 tumour-bearing nude mouse (Fig. 7A), the black arrows indicate the

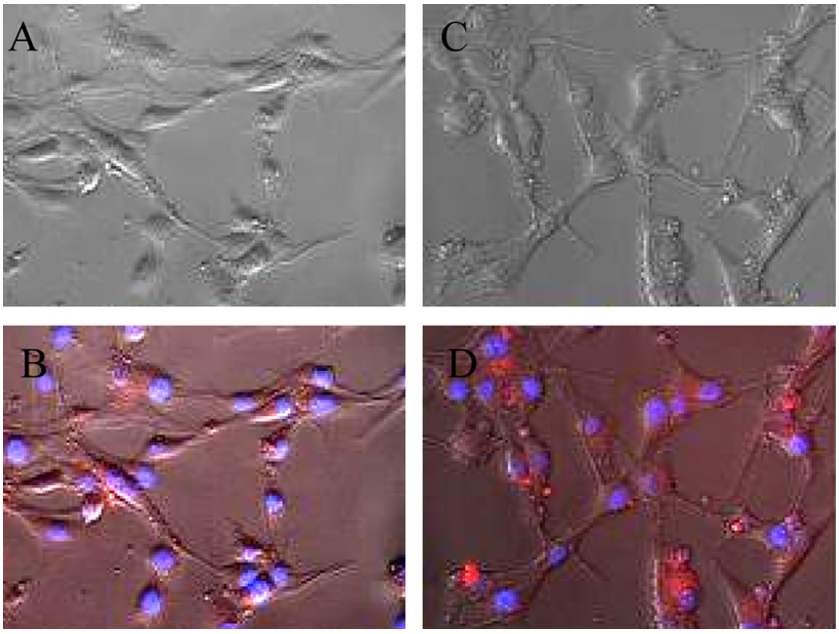

Fig. 3. Cellular uptake of the mPEG–PEI/pGL$_{4.2}$ (A and B) and RGERPPR–PEG–PEI/pGL$_{4.2}$ (C and D), complexes in U87 glioma cells. Images were taken on a fluorescence microscope following a 4 h period of incubation. The cell nuclei were stained with DAPI (blue), and the pDNA was labelled with TOTO®-3 (red). Original magnification: 400×. (For interpretation of the references to color in text, the reader is referred to the web version of this article.)

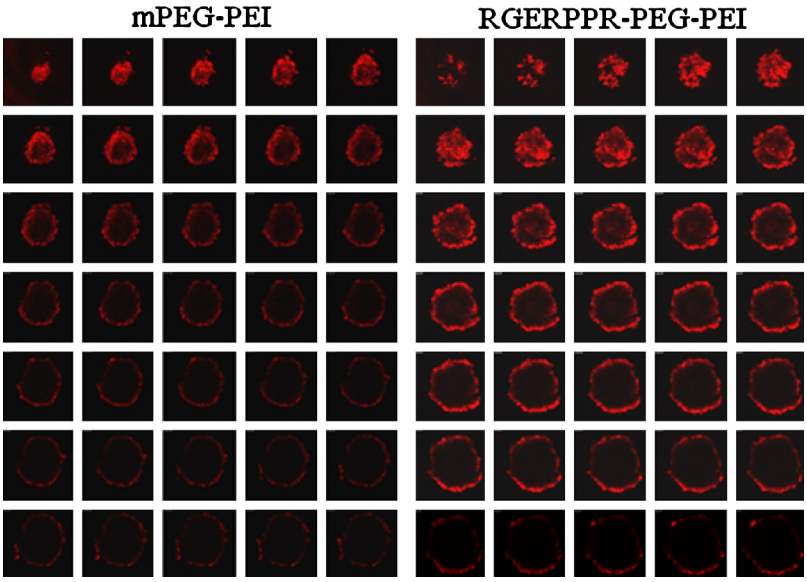

Fig. 4. U87 tumour spheroid penetration analyses of mPEG–PEI/pGL$_{4.2}$ and RGERPPR–PEG–PEI/pGL$_{4.2}$. The plasmid DNA (pGL4.2) was labelled with TOTO®-3. Both figures are multi-level scans of the penetration of the complexes. The interval between consecutive slides was 5 μm. Original magnifications: 200×.

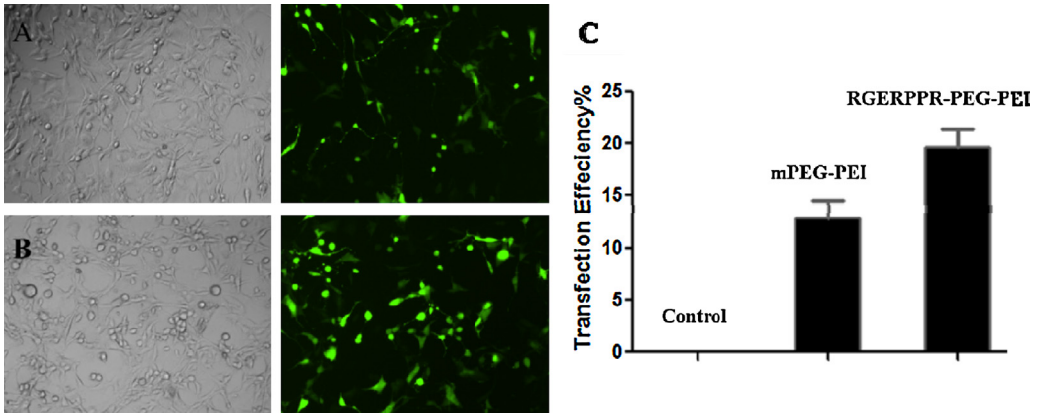

Fig. 5. Fluorescent images of the gene expression of (A) mPEG–PEI/pEGFP-N2 and (B) RGERPPR–PEG–PEI/pEGFP-N2 in U87 glioma cells at an *N*/*P* ratio of 12. (C) Quantitative evaluation of the EGFP expression by flow cytometry. Original magnification: 200×.

tumour tissue area, whereas the yellow arrows are used to indicate the normal tissue area, and the red line the boundary between the two kinds of tissue. Based on these results, it was concluded that the intracranial glioblastoma model had been successfully established.

To evaluate the targeting potency of RGERPPR–PEG–PEI in vivo, a red fluorescence protein assay was conducted in the mice of the intracranial U87 glioblastoma model. The in vitro transfection

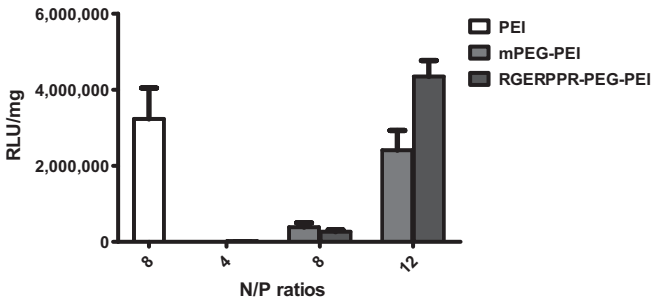

Fig. 6. Luciferase expression levels in U87 glioma cells at different *N*/*P* ratios (polymer/pGL$_{4.2}$); the PEI (25 kDa) control was used with the optimal *N*/*P* ratio of 8. $^{*}P < 0.05$, significantly different.

results revealed that RGERPPR–PEG–PEI attained a maximum level of transfection efficiency at an *N*/*P* ratio of 12. An *N*/*P* ratio of 12 was therefore subsequently selected for in vivo evaluation. As shown in Fig. 7B and C, the RGERPPR–PEG–PEI/pDsRED-N1 complex led to a higher relative level of fluorescent intensity than that of mPEG–PEI. For the RGERPPR–PEG–PEI complex, the sum intensity in brain was 6.26-fold higher than that of the mPEG–PEI. These results therefore indicated a significant increase in the levels of red fluorescence protein expression.

4. Discussion

GBM is the most common and aggressive malignant brain tumour in humans with an average survival time of about one year (Jain et al., 2007). Unfortunately, however, the existing treatments for this disease do not provide significant increases in survival, despite recent advances in multimodality therapies, and research in this area towards the development of innovative therapeutic strategies remains challenging (Lima et al., 2012). To overcome the problems associated with the blood–tumour barrier (BTB) in the treatment of brain tumours, a strategy involving the introduction of ligands that specifically bind to brain tumour cell receptors

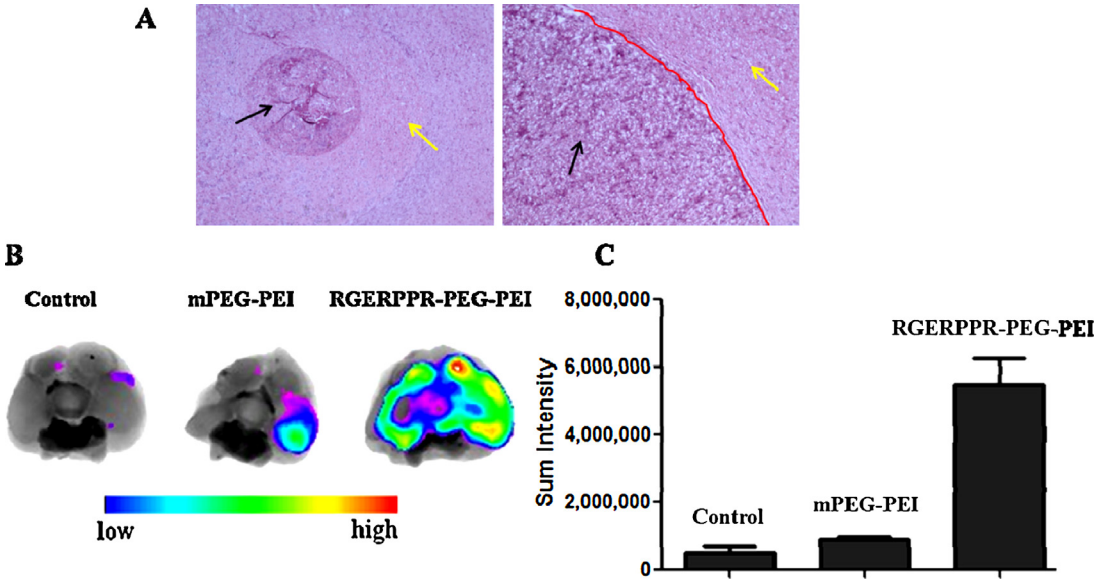

Fig. 7. (A) Histological characteristics of the U87 glioblastoma in the brain of a nude mouse (sections were stained with H&E); (B) Fluorescent imaging of mPEG–PEI/pDsRED-N1 and RGERPPR–PEG–PEI/pDsRED-N1 in the brains of nude mice bearing U87 glioblastoma. The images measured using a fluorescent imaging system. (C) Quantitative evaluation of RFP expression in the brains.

could be particularly advantageous (Zhan et al., 2010; Gao et al., 2012a,b; Gu et al., 2013), because the BTB becomes the main obstacle to anti-glioma drug delivery systems during the development of brain tumours and the associated gradual impairment of the BBB (Gerstner and Batchelor, 2012).

In the current study, a brain tumour binding and tissue-penetrating CendR peptide RGERPPR was conjugated with branched PEI via heterobifunctional PEG to give an RGERPPR–PEG–PEI polymer for intracranial GBM-targeted gene delivery. The degree of substitution and molecular weight properties of the resulting mPEG–PEI and RGERPPR–PEG–PEI complexes were verified by ^{1}H NMR, and determined to be 4.30 and 33.6 kDa, and 4.39 and 37.1 kDa, respectively. Analysis of the sizes and zeta potentials indicated that the PEGylated complexes were capable of binding plasmid DNA and condensing DNA into small positive nanoparticles.

An important issue for the systemic delivery of therapeutic genes in clinical applications is the requirement for high levels of efficiency in the targeted vectors, as well as minimum side effect. As shown by the results of the cytotoxicity assay, the PEGylation of the PEI complexes led to a reduction in their cytotoxicities, as well as an increase in the cell viability levels because of the shielding effect of PEG (Nguyen et al., 2000; Petersen et al., 2002), and these properties represent important advantages in terms of potential in vivo applications. In vitro qualitative and quantitative assays revealed a significant increase in the transfection efficiency of RGERPPR–PEG–PEI/pGL$_{4.2}$ relative to the non-targeted polymer. The current results were attributed in part to the enhanced U87 glioma cell uptake of RGERPPR–PEG–PEI/pGL$_{4.2}$ (Fig. 3), which resulted from the specific binding and internalisation ability of RGERPPR, because RGERPPR (CendR peptide) has been reported to exhibit a high binding affinity to the NRP-1 receptor, which is also over-expressed in U87 glioma cells (Osada et al., 2004; Nasarre et al., 2010; Li et al., 2011).

Tumour targeted anti-cancer drugs and genes delivery systems have become significant strategies for the treatment of cancer, because they can be used to specifically target tumour cells and improve drug delivery, respectively. Dysfunctional tumour blood vessels and high levels of interstitial pressure in the tumour parenchyma, however, can lead to poor penetration efficacy in drugs, genes and nanoparticles, and overcoming the resulting reduced levels of treatment efficacy remains a major challenge (Heldin et al., 2004). CendR peptides have been reported that can increase vascular permeability and penetrate tumour tissues by binding to NRP-1, and these properties have provided a way to overcome high levels of interstitial pressure in tumours (Teesalu et al., 2009). Based on these current levels of understanding, the CendR peptide RGERPPR was used in the current study to improve the penetrating activity of mPEG–PEI. The results revealed that the RGERPPR–PEG–PEI/pDsRED-N1 complex provided a significant increase in the levels of red fluorescence protein expression in the brains of intracranial U87 glioblastoma-bearing nude mice. These results were attributed to the targeting potency of the complex towards the U87 glioma cells and the increased level of penetrating activity into the tumour tissues of RGERPPR (Fig. 4). Both of these factors played important roles in enhancing the overall accumulation of genes within the tumour, and therefore led to an increase in the transfection efficiency relative to the non-targeted mPEG–PEI.

5. Conclusions

In conclusion, we have developed a novel targeted non-viral gene vector bearing the NRP-1 recognition peptide RGERPPR. The resulting RGERPPR–PEG–PEI was characterised by ^{1}H-NMR and then used to condense a plasmid gene. Compared with PEI/pDNA, RGERPPR–PEG–PEI/pDNA provided a significant increase in transfection efficiency in glioblastoma U87 glioma cells both in vitro and in vivo, as well as affording reduced levels of cytotoxicity. Based on these results, the RGERPPR peptide has been identified as a suitable candidate ligand for targeting the NRP-1 receptor, with potential application in the treatment of glioblastoma.

Conflict of interest statement

The authors declare no competing financial interest.

Acknowledgments

This work was supported by the National Key Basic Research Program of China (Grant Nos. 2013CB932502 and 2010CB934000), the National Science and Technology Major Project (Grant No.

2012ZX09304004), the National Science Foundation of China (Grant Nos. 30772655 and 81202471), the Foundation Program of the Key Laboratory of Smart Drug Delivery of the Ministry of Education, and the Foundation Program of Key Laboratory of Smart Drug Delivery of the Ministry of Education (SDD2011-03). We would also like to thank our reviewers for their helpful comments.

References

Bai, C.Z., Choi, S., Nam, K., An, S., Park, J., 2013. Arginine modified PAMAM dendrimer for interferon beta gene delivery to malignant glioma. Int. J. Pharm. 445, 79–87.
Boussif, O., Lezoualch, F., Zanta, M.A., Mergny, M.D., Scherman, D., Demeneix, B., Behr, J.P., 1995. A versatile vector for gene oligonucleotide transfer into cells in culture and in vivo: polyethylenimine. Proc. Natl. Acad. Sci. U. S. A. 92, 7297–7301.
Gao, H.L., Qian, J., Cao, S.J., Yang, Z., Pang, Z.Q., Pan, S.Q., Fan, L., Xi, Z.J., Jiang, X.G., Zhang, Q.Z., 2012a. Precise glioma targeting of and penetration by aptamer and peptide dual-functioned nanoparticles. Biomaterials 33, 5115–5123.
Gao, H., Qian, J., Yang, Z., Pang, Z., Zhang, S., Zhang, Q., 2012b. Whole-cell SELE X aptamer-functionalised poly(ethyleneglycol)–poly(ε-caprolactone) nanoparticles for enhanced targeted glioblastoma therapy. Biomaterials 33, 6264–6272.
Gerstner, E.R., Batchelor, T.T., 2012. Antiangiogenic therapy for glioblastoma. Cancer J. 18, 45–50.
Gladson, C.L., Prayson, R.A., Liu, W.M., 2010. The pathobiology of glioma tumors. Annu. Rev. Pathol. 5, 33–50.
Godbey, W.T., Wu, K.K., Mikos, A.G., 1999. Poly(ethylenimine) and its role in gene delivery. J. Control. Release 60, 149–160.
Groothuis, D.R., 2000. The blood–brain and blood–tumor barriers: a review of strategies for increasing drug delivery. Neuro-Oncology 2, 45–59.
Gu, G., Gao, X., Hu, Q., Kang, T., Liu, Z., Jiang, M., Miao, D., Song, Q., Yao, L., Tu, Y., Pang, Z., Chen, H., Jiang, X., Chen, J., 2013. The influence of the penetrating peptide iRGD on the effect of paclitaxel-loaded MT1-AF7p-conjugated nanoparticles on glioma cells. Biomaterials 34, 5138–5148.
He, Z.G., TessierLavigne, M., 1997. Neuropilin is a receptor for the axonal chemorepellent Semaphorin III. Cell 90, 739–751.
Heldin, C., Rubin, K., Pietras, K., Östman, A., 2004. High interstitial fluid pressure—an obstacle in cancer therapy. Nat. Rev. Cancer 4, 806–813.
Hu, Q.Y., Gu, G.Z., Liu, Z.Y., Jiang, M.Y., Kang, T., Miao, D.Y., Tu, Y.F., Pang, Z.Q., Song, Q.X., Yao, L., Xia, H.M., Chen, H.Z., Jiang, X.G., Gao, X.L., Chen, J., 2013. F3 peptide-functionalized PEG-PLA nanoparticles co-administrated with tLyp-1 peptide for anti-glioma drug delivery. Biomaterials 34, 1135–1145.
Jain, R.K., Di Tomaso, E., Duda, D.G., Loeffler, J.S., Sorensen, A.G., Batchelor, T.T., 2007. Angiogenesis in brain tumours. Nat. Rev. Neurosci. 8, 610–622.
Kleemann, E., Neu, M., Jekel, N., Fink, L., Schmehl, T., Gessler, T., Seeger, W., Kissel, T., 2005. Nano-carriers for DNA delivery to the lung based upon a TAT-derived peptide covalently coupled to PEG–PEI. J. Control. Release 109, 299–316.
Kolodkin, A.L., Levengood, D.V., Rowe, E.G., Tai, Y.T., Giger, R.J., Ginty, D.D., 1997. Neuropilin is a Semaphorin III receptor. Cell 90, 753–762.
Li, X.Y., Tang, T., Lu, X.Z., Zhou, H.G., Huang, Y.Y., 2011. RNA interference targeting NRP-1 inhibits human glioma cell proliferation and enhances cell apoptosis. Mol. Med. Rep. 4, 1261–1266.
Lima, F., Kahn, S.A., Soletti, R.C., Biasoli, D., Alves, T., Da Fonseca, A., Garcia, C., Romao, L., Brito, J., Holanda-Afonso, R., Faria, J., Borges, H., Moura-Neto, V., 2012. Glioblastoma: therapeutic challenges, what lies ahead. BBA – Rev. Cancer 1826, 338–349.
Lopes, M.B.S., 2003. Angiogenesis in brain tumors. Microsc. Res. Tech. 60, 225–230.
Lungwitz, U., Breunig, M., Blunk, T., Gopferich, A., 2005. Polyethylenimine-based non-viral gene delivery systems. Eur. J. Pharm. Biopharm. 60, 247–266.
Luo, X., Pan, S.R., Feng, M., Wen, Y.T., Zhang, W., 2010. Stability of poly(ethylene glycol)-graft-polyethylenimine copolymer/DNA complexes: influences of PEG molecular weight and PEGylation degree. J. Mater. Sci. Mater. Med. 21, 597–607.
Merkel, O.M., Germershaus, O., Wada, C.K., Tarcha, P.J., Merdan, T., Kissel, T., 2009. Integrin alphaVbeta3 targeted gene delivery using RGD peptidomimetic conjugates with copolymers of PEGylated poly(ethylene imine). Bioconjug. Chem. 20, 1270–1280.
Meyer, M.A., 2008. Malignant gliomas in adults. N. Engl. J. Med. 359, 1850-1850.
Mickler, F.M., Vachutinsky, Y., Oba, M., Miyata, K., Nishiyama, N., Kataoka, K., Brauchle, C., Ruthardt, N., 2011. Effect of integrin targeting and PEG shielding on polyplex micelle internalization studied by live-cell imaging. J. Control. Release 156, 364–373.
Murphy, A.M., Rabkin, S.D., 2013. Current status of gene therapy for brain tumors. Transl. Res. 161, 339–354.
Nasarre, C., Roth, M., Jacob, L., Roth, L., Koncina, E., Thien, A., Labourdette, G., Poulet, P., Hubert, P., Cremel, G., Roussel, G., Aunis, D., Bagnard, D., 2010. Peptide-based interference of the transmembrane domain of neuropilin-1 inhibits glioma growth in vivo. Oncogene 29, 2381–2392.
Neu, M., Fischer, D., Kissel, T., 2005. Recent advances in rational gene transfer vector design based on poly(ethylene imine) and its derivatives. J. Gene Med. 7, 992–1009.
Neu, M., Germershaus, O., Behe, M., Kissel, T., 2007. Bioreversibly crosslinked polyplexes of PEI and high molecular weight PEG show extended circulation times in vivo. J. Control. Release 124, 69–80.
Nguyen, H.K., Lemieux, P., Vinogradov, S.V., Gebhart, C.L., Guerin, N., Paradis, G., Bronich, T.K., Alakhov, V.Y., Kabanov, A.V., 2000. Evaluation of polyether–polyethyleneimine graft copolymers as gene transfer agents. Gene Ther. 7, 126–138.
Ogris, M., Brunner, S., Schuller, S., Kircheis, R., Wagner, E., 1999. PEGylated DNA/transferrin–PEI complexes: reduced interaction with blood components, extended circulation in blood and potential for systemic gene delivery. Gene Ther. 6, 595–605.
Oh, H., Takagi, H., Otani, A., Koyama, S., Kemmochi, S., Uemura, A., Honda, Y., 2002. Selective induction of neuropilin-1 by vascular endothelial growth factor (VEGF): a mechanism contributing to VEGF-induced angiogenesis. Proc. Natl. Acad. Sci. U. S. A. 99, 383–388.
Osada, H., Tokunaga, T., Nishi, M., Hatanaka, H., Abe, Y., Tsugu, A., Kijima, H., Yamazaki, H., Ueyama, Y., Nakamura, M., 2004. Overexpression of the neuropilin 1 (NRP1) gene correlated with poor prognosis in human glioma. Anticancer Res. 24, 547–552.
Pardridge, W.M., 2002. Drug and gene delivery to the brain: the vascular route. Neuron 36, 555–558.
Petersen, H., Fechner, P.M., Martin, A.L., Kunath, K., Stolnik, S., Roberts, C.J., Fischer, D., Davies, M.C., Kissel, T., 2002. Polyethylenimine-graft-poly(ethylene glycol) copolymers: influence of copolymer block structure on DNA complexation and biological activities as gene delivery system. Bioconjug. Chem. 13, 845–854.
Roth, L., Agemy, L., Kotamraju, V.R., Braun, G., Teesalu, T., Sugahara, K.N., Hamzah, J., Ruoslahti, E., 2012. Transtumoral targeting enabled by a novel neuropilin-binding peptide. Oncogene 31, 3754–3763.
Soker, S., Miao, H.Q., Nomi, M., Takashima, S., Klagsbrun, M., 2002. VEGF(165) mediates formation of complexes containing VEGFR-2 and neuropilin-1 that enhance VEGF(165)-receptor binding. J. Cell. Biochem. 85, 357–368.
Soker, S., Takashima, S., Miao, H.Q., Neufeld, G.K., lagsbrun, M., 1998. Neuropilin-1 is expressed by endothelial and tumor cells as an isoform-specific receptor for vascular endothelial growth factor. Cell 92, 735–745.
Sugahara, K.N., Teesalu, T., Karmali, P.P., Kotamraju, V.R., Agemy, L., Girard, O.M., Hanahan, D., Mattrey, R.F., Ruoslahti, E., 2009. Tissue-penetrating delivery of compounds and nanoparticles into tumors. Cancer Cell 16, 510–520.
Sugahara, K.N., Teesalu, T., Karmali, P.P., Kotamraju, V.R., Agemy, L., Greenwald, D.R., Ruoslahti, E., 2010. Co-administration of a tumor-penetrating peptide enhances the efficacy of cancer drugs. Science 328, 1031–1035.
Takahashi, T., Fournier, A., Nakamura, F., Wang, L.H., Murakami, Y., Kalb, R.G., Fujisawa, H.S., Trittmatter, S.M., 1999. Plexin–neuropilin-1 complexes form functional semaphorin-3A receptors. Cell 99, 59–69.
Teesalu, T., Sugahara, K.N., Kotamraju, V.R., Ruoslahti, E., 2009. C-end rule peptides mediate neuropilin-1-dependent cell, vascular, and tissue penetration. Proc. Natl. Acad. Sci. U. S. A. 106, 16157–16162.
Zhan, C.Y., Gu, B., Xie, C., Li, J., Liu, Y., Lu, W.Y., 2010. Cyclic RGD conjugated poly(ethylene glycol)-co-poly(lactic acid) micelle enhances paclitaxel anti-glioblastoma effect. J. Control. Release 143, 136–142.
Zhan, C.Y., Wei, X.L., Qian, J., Feng, L.L., Zhu, J.H., Lu, W.Y., 2012. Co-delivery of TRAIL gene enhances the anti-glioblastoma effect of paclitaxel in vitro and in vivo. J. Control. Release 160, 630–636.